Behavior of explosive bubbles behind an underwater shock wave

N. Watanabe, K. Ishii
Department of Mechanical Engineering, Yokohama National University
79-5 Tokiwadai, Hodogaya-ku, Yokohama 240-8501, Japan

1 Introduction

A combustion phenomenon that oxyhydrogen bubbles arranged in line in glycerol burn sequentially with propagation of a pressure wave was demonstrated by Hasegawa and Fujiwara, who named such series of explosion bubble detonation [1]. Afterwards it has been studied experimentally and theoretically by several researchers. Sychev and Pinaev found that the bubble detonation is a self-sustainable soliton wave on the basis of their experimental study on its initiation conditions [2]. Trotsyuk and Fomin modeled the bubble detonation and their calculated results show good agreement with the experimental results in propagation speed and time when the bubbles start to react [3].

On the other hand, it is known that an inert gas bubble in liquid behind a shock wave shrinks and then expands, generating a spherical shock wave in turning to expansion. In the case of the bubble detonation, explosive bubbles are expected to generate stronger shock waves than inert bubbles, because the self-sustained pressure wave is not formed in inert bubbly medium [4]. Until now, a pressure history of the shock wave generated by a single explosive bubble has not been experimentally measured as far as the author knows. The pressure measurement near the bubble is useful to verify self-sustained mechanism of bubble detonation. In addition, local high pressure is applicable to sterilization using shock waves proposed recently [5].

In the present work, an underwater shock wave driven by gaseous detonation propagates in water containing explosive gas bubbles. Behavior of the explosive bubbles behind the underwater shock wave was experimentally studied. Special care has been taken on measurement of pressure generated from expansion of the single explosive bubble.

2 Experimental Apparatus

A schematic of experimental apparatus is shown in Fig. 1. It consists of three parts; a detonation tube, an imploding section, and a test section. The detonation tube has an inner diameter of 100 mm and a length of 1032 mm. As for the imploding section of 68 mm in length, its inner diameter gradually changes from 100

Correspondence to: ishii-kazuhiro-rh@ynu.ac.jp

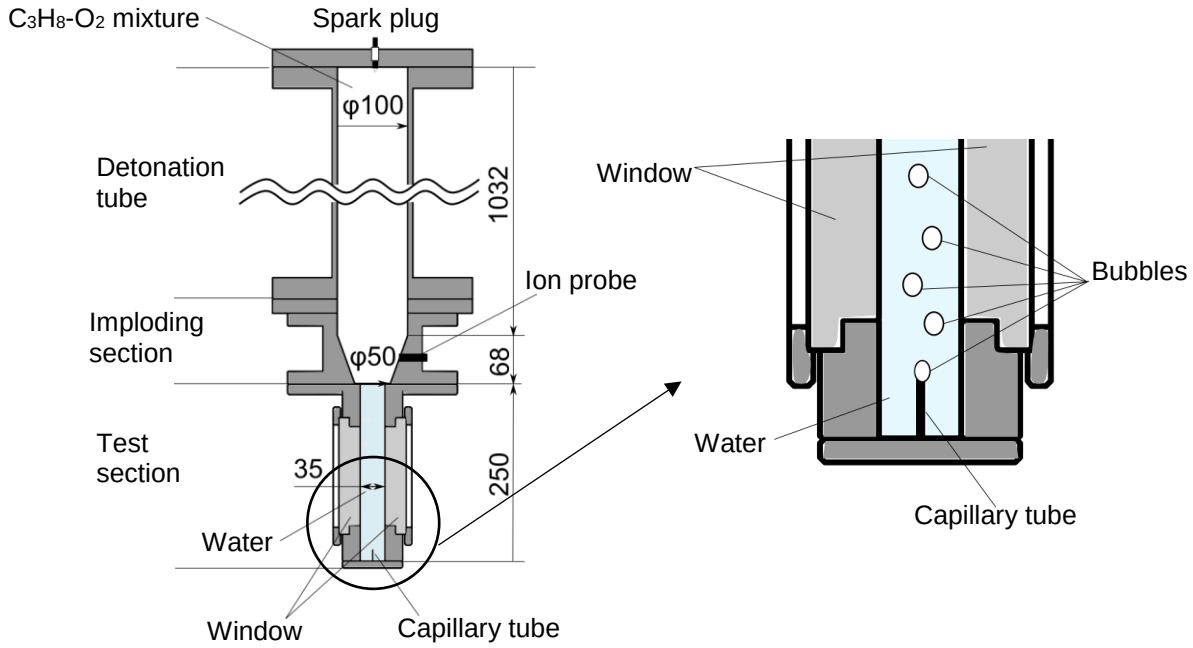

Fig. 1. Schematic of experimental apparatus.

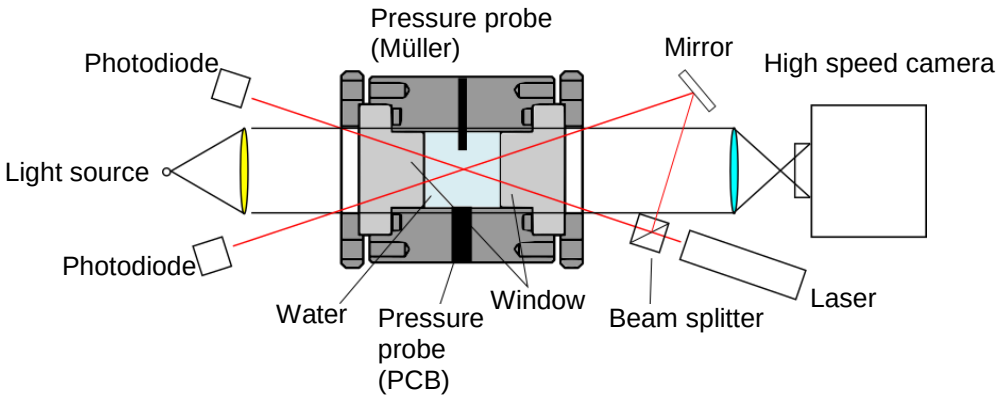

Fig. 2. Optical setup.

mm to 50 mm. The test section has 35 mm square cross section and a length of 250 mm. In operation, the detonation tube and the imploding section are initially charged with a stoichiometric C_3H_8-O_2 mixture, while the test section is filled with water. Bubbles are introduced from a capillary tube placed at the bottom of the test section (see right in Fig. 1). The bubbles are made of a stoichiometric C_2H_4-O_2 mixture. Initial equivalent diameter of the introduced bubbles ranges from 2 mm to 4 mm. When two laser beams shown in Fig. 2 are intercepted by a bubble at the observation position, the mixture in the detonation tube is ignited by a spark plug placed at the upper end. After deflagration-to-detonation process, the detonation wave then propagates downward, the shock wave is reflected on the water surface, and a transmitted shock wave travels in the water. Although the bubble moves upward in the water due to buoyancy, moving speed of the bubble is

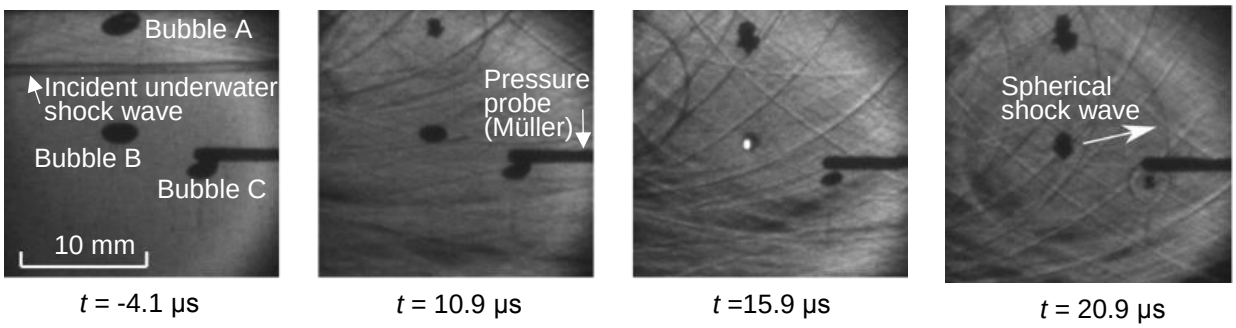

Fig. 3. High speed images of explosive bubble behavior.

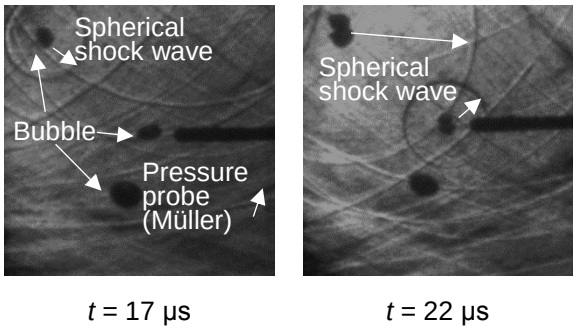

Fig. 4. Generation of spherical shock wave by explosive bubble.

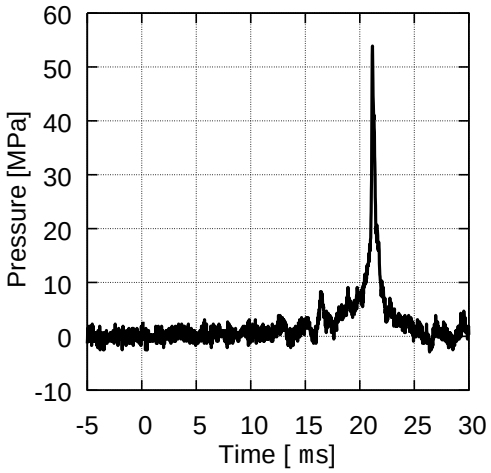

Fig. 5. Typical pressure history in shock-bubble interaction.

much slower than the DDT process and the following detonation wave. Movement of the bubble, therefore, is negligible so that the bubble can be assumed to stay at the observation position when the underwater shock wave acts on it. The spherical shock wave generated by the bubble expansion is visualized by the shadowgraph method. An optical setup for shadowgraph is shown in Fig. 2. In addition, two kinds of pressure probes (PCB M109C and Müller-Platte needle probe) are installed at the observation position. The pressure increase behind the incident underwater shock wave was measured with the former, while the pressure rise induced by the spherical shock wave due to the bubble expansion was measured with the latter. Sensitivity of the latter is strongly dependent on the relative direction of pressure waves to the probe and becomes highest when the wavefront is normal to the probe axis.

3 Results and Discussion

Overall behavior of the explosive bubbles behind the incident underwater shock wave is shown in Fig. 3. At t = - 4.1 μs, the incident shock wave and three bubbles (A~C) can be observed around the probe. t = 0 μs is a time when the incident shock wave reaches the bubble B. After the incident shock wave passes away, the bubble B starts to shrink. A self-emission from it is then observed at t = 15.9 μs, indicating that

combustion of the mixture in the bubble occurs. Afterwards a spherical shock wave generated by expansion of the bubble B can be seen at t = 20.9 μs. Its initial equivalent radius of the bubble, R_0 was about 1.3 mm and the peak pressure behind the incident shock wave, P_i was about 3.9 MPa. Rayleigh's bubble collapse time, $t_{collapse}$ given by Eq. (1) is estimated to be 19 μs, which is the same order of magnitude as the shrinking time in the experiment,

$$t_{collapse} = 0.915 R_0 \sqrt{\frac{\rho_l}{p_i}}, \qquad (1)$$

where ρ_l is density of the water [6].

Generation of the spherical shock wave by the bubble expansion is displayed in Fig. 4. Figure 5 shows the pressure history measured with the Müller pressure probe in the same test as of Fig. 4. Although time of zero means the arrival time of the incident shock wave, almost no pressure rise can be found at t = 0 μs in Fig. 5. This is due to the angle dependence of the probe sensitivity, because the wavefront of the incoming incident shock wave is parallel to the probe axis. According to the images in Fig. 4, a spherical shock wave is generated by the bubble whose center is on the probe axis and reaches the probe between t = 17 μs and 22 μs. In Fig. 5, the peak pressure of 53.9 MPa is obtained at t = 21 μs and it is found that this peak pressure is due to the spherical shock wave generated by the bubble. The influence of shock waves generated by bubbles located relatively far from the pressure probe, the measured peak pressure is treated as the shock wave pressure generated by the nearest bubble. The distance between the nearest bubble and the probe, d is 2.0 mm in these images.

From these high speed images and the pressure profiles, relationship between the peak pressure and the distance d is obtained as shown in Fig. 6, where d^* (= d / R_0) is dimensionless distance. The peak pressure, P_{peak} decreases with increase in d^*. The maximum value of P_{peak} of 53.9 MPa is obtained for d^* = 1.4. However, there is a possibility of underestimating the peak pressure because of the angle dependence of the probe sensitivity mentioned above. This uncertainty of the bubble position leads to the scattered plots as shown in Fig.6.

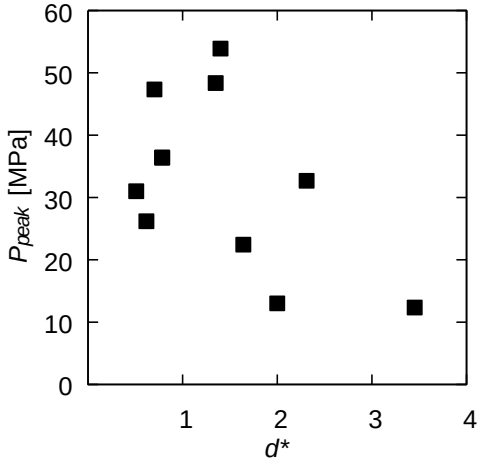

Fig. 6. Relation between peak pressure of shock wave due to bubble expansion and dimensionless distance d*.

To estimate the area influenced by the bubble expansion, a ratio of the peak pressure of the bubble-generated shock wave to that of the incident underwater shock wave is plotted against d^* as shown in Fig. 7. This pressure ratio over unity is obtained for d^* < 2.5 and has a maximum value of 5.3.

Figure 8 shows the modified peak shock pressure with correction of the angle dependence of the probe sensitivity. Here, uncertainty of the bubble position in the depth direction was estimated from the laser beam diameter and the initial bubble radius. Briefly, the maximum angle between a bubble and the probe center was calculated when a bubble could be detected by the laser beam, and then the measured peak pressure was corrected by using the angle-sensitivity relation of the probe provided by the manufacturer.

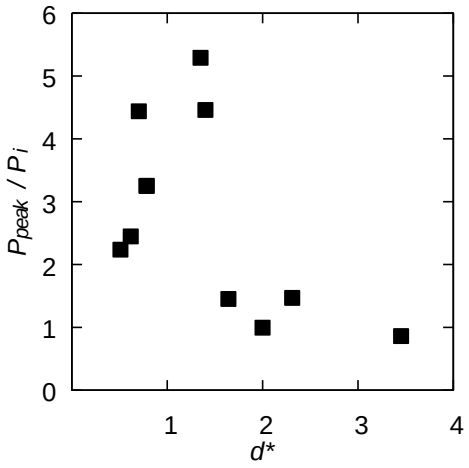

Fig. 7. Ratio of peak pressure of shock wave due to bubble expansion to that behind incident underwater shock wave.

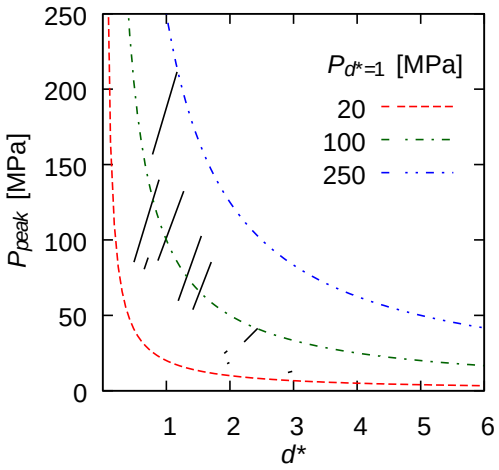

Fig. 8. Modified peak pressure of shock wave caused by bubble expansion with correction of angle dependence of sensitivity of the pressure probe.

Consequently the maximum values of the peak pressure shown in Fig. 8 are different from those in Fig. 6. The right upper end of each plot shows the case where the bubble position deviates most in the depth direction and the influence of the angle is the largest. The left end of each plot shows the case in which the bubble center is assumed to be located on the same plane with the probe and the correction factor becomes the smallest. Since the peak pressure of the bubble-generated shock wave is inversely proportional to the distance between the bubble and the measurement position [6], a curve expressed by the following equation is shown in Fig. 8,

$$P_{d^*=1} = P_{peak} \times d^*, \tag{2}$$

where, $P_{d*=1}$ denotes the peak pressure for $d = R_0$, namely $d^* = 1$. The experimental results show that $P_{d*=1}$ is in the range of 20~250 MPa. In the present work, $P_{d*=1}$ is not fixed to one value because there is variation in P_i, where average value is 14.0 ± 4.4 MPa.

4 Summary

In the present work, underwater shock wave driven by detonation propagates in water containing explosive bubbles made of a stoichiometric C_2H_4-O_2 mixture.

1) Behind the underwater shock wave, the bubble startes to shrink resulting in combustion, and then expands, which is followed by generation of a spherical shock wave.

2) The maximum pressure of 54 MPa is obtained at a distance of 2.0 mm from the bubble after the shock-bubble interaction.

3) The peak pressure caused by the bubble expansion is approximately inversely proportional to the distance from the bubble and shows higher values than that behind the underwater shock wave, if the distance is within about 2.5 times the initial bubble radius.

Acknowledgments

This work was supported by Tanikawa Fund Promotion of Thermal Technology 2015 and JSPS KAKENHI Grant Number JP16K14712.

References

[1] Hasegawa T, Fujiwara T. (1982). Detonation in oxyhydrogen bubbled liquids. Proceeding of the Symposium (International) on Combustion 19: 675-683.

[2] Sychev AI, Pinaev AV. (1986). Self-sustaining detonation in liquids with bubbles of explosive gas. Journal of Applied Mechanics and Technical Physics 27(1): 119-123

[3] Trotsyuk AV, Fomin PA. (1992). Model of Bubble detonation. Combustion, Explosion and Shock Waves 28(4): 439-445

[4] Kochetcov II. Pinaev AV. (2013). Comparative characteristics of strong shock and detonation waves in bubble media by an electrical wire explosion. Shock Waves 23 : 139-152

[5] Abe A , Mimura H , Ishida H, Yoshida K. (2007).The effect of shock pressures on the inactivation of a marine Vibrio sp. Shock Waves 17: 143-151

[6] Brennen CE. (1995) Cavitation and bubble dynamics. Oxford University Press (ISBN 0-19-509409-3)